Journal of NeuroEngineering and Rehabilitation

RESEARCH

Open Access

A machine learning approach for the design optimization of a multiple magnetic and inertial sensors wearable system for the spine mobility assessment

Dalia Y. Domínguez-Jiménez[1], Adriana Martínez-Hernández[2*], Gustavo Pacheco-Santiago[1], Julio C. Casasola-Vargas[3,4], Rubén Burgos-Vargas[3] and Miguel A. Padilla-Castañeda[1*]

Abstract

Background Recently, magnetic and inertial measurement units (MIMU) based systems have been applied in the spine mobility assessment; this evaluation is essential in the clinical practice for diagnosis and treatment evaluation. The available systems are limited in the number of sensors, and neither develops a methodology for the correct placement of the sensors, seeking the relevant mobility information of the spine.

Methods This work presents a methodology for analyzing a system consisting of sixteen MIMUs to reduce the amount of information and obtain an optimal configuration that allows distinguishing between different body postures in a movement. Four machine learning algorithms were trained and assessed using data from the range of motion in three movements (Mov.1—Anterior hip flexion; Mov.2—Lateral trunk flexion; Mov.3—Axial trunk rotation) obtained from 12 patients with Ankylosing Spondylitis.

Results The methodology identified the optimal minimal configuration for different movements. The configuration showed good accuracy in discriminating between different body postures. Specifically, it had an accuracy of 0.963 ± 0.021 for detecting when the subject is upright or bending in Mov.1, 0.944 ± 0.038 for identifying when the subject is flexed to the left or right in Mov.2, and 0.852 ± 0.097 for recognizing when the subject is rotated to the right or left in Mov.3.

Conclusions Our results indicate that the methodology developed results in a feasible configuration for practical clinical studies and paves the way for designing specific IMU-based assessment instruments.

Trial registration: Study approved by the Local Ethics Committee of the General Hospital of Mexico "Dr. Eduardo Liceaga" (protocol code DI/03/17/471).

Keywords Inertial measurement units, Spine, Biomechanics, Machine learning, Musculoskeletal Disorders

*Correspondence:
Adriana Martínez-Hernández
adriana.martinez@ibero.mx
Miguel A. Padilla-Castañeda
miguel.padilla@icat.unam.mx
Full list of author information is available at the end of the article

Introduction

Spine mobility assessment is part of clinical practice in some areas like rheumatology, orthopedics, and rehabilitation; this evaluation is essential for the diagnosis, Lemeunier et al. [1] present the clinical assessment of the cervical spine's posture, mobility, and its associated disorders. Besides, this mobility assessment helps clinicians to evaluate the patient's progress, Sieper et al. [2] developed a handbook to assess Ankylosing Spondylitis (AS) patients; this rheumatic condition affects the lumbar spine and the sacroiliacs articulations primordially. In other areas like orthopedics and neurology, spine mobility evaluation attends to verify the pre and post-surgery results [3]. Despite the importance of this procedure, metrics are obtained with measuring tape and goniometers, as in the case of AS patient's evaluation where the index BASMI (Bath Ankylosing Spondylitis Metrology Index) is applied with the instruments mentioned above [4]. Moreover, in many cases, in areas like orthopedics and rehabilitation, the evaluation is through palpation and medical observation [5]; thus, some studies have demonstrated that measurements obtained with manual methods lack accuracy, sensibility, and repeatability [6–8].

In addition, mobility assessment is focused mainly on the lumbar and cervical spine, leaving behind the thoracic spine [9–11] despite thoracic vertebrae contributing to upper limb movements and, in some cases, thoracic affection can limit lung capacity [12, 13]. For all these, it is crucial to use technological tools to improve the assessment of the entire spine at lumbar, thoracic, and cervical levels, with accuracy, sensibility, and in more range of motion (RoM), unable to evaluate with the existing manual tools.

Systems based on magnetic and inertial measurement units (MIMUs) have proven their reliability and precision in the analysis of human movement, applied in several clinical areas. Kortier et al. [14] proposed a system that allows a 3D reconstruction of the hand to analyze the functionality of these complex joints. A system for the elderly population was proposed by Nguyen et al. [15] to detect daily physical activities. Revi et al. [16] presented a method for gait analysis to detect locomotion functionality in neurological patients. Furthermore, MIMUs have been applied in areas like rehabilitation [17], rheumatism [18], and ergonomics [19].

Recently, MIMU-based systems have been applied in the evaluation of spine mobility, showing great feasibility [20, 21]; since these systems allow their use without limiting patients' mobility, they can measure the continuous variation of angles [22], and the use of controlled environments like those used with optical systems are not necessary [23, 24]. However, the systems mentioned above are limited in the number of sensors to evaluate the entire spine; they generally use two sensors to evaluate the lumbar spine and two for the cervical spine, leaving behind the thoracic area [10, 11, 25]. Franco et al. [26] use six sensors along the entire spine, but neither of these works develops a methodology for the correct placement of the sensors, seeking the most relevant mobility information of the spine.

In a previous work [27, 28], the authors reported the development of a wearable system based on MIMUs designed explicitly for the mobility assessment of the spine, particularly for patients suffering from Ankylosing Spondylitis [29, 30]. The system consists of 16 MIMUs that, through Kalman filters, estimate the kinematic orientation of 16 individual segments located at the patient's spine. The system's reliability has been validated in 15 healthy subjects who performed a group of six exercises involving the mobility of the entire spine, with the MIMUs located serially along the subject's back, as illustrated in Fig. 1a. The exercises evaluated were anterior hip flexion, trunk lateral flexion, trunk axial rotation, cervical axial rotation, cervical flexion/extension, and cervical lateral flexion. To the best of our knowledge, this system is the only one capable of monitoring different movements of the lumbar, thoracic, and cervical areas simultaneously, with several degrees of freedom.

The tests revealed the high reliability of the system, observed in the intraclass correlation coefficients (ICC) [31] of every MIMU individually and globally for five of the six movements [27]. For the axial trunk rotation movement, mid to low ICCs were observed at some locations, mainly due to the sensors' erratic motions owing to the participants' skin displacement. Thus, despite the possibilities offered by the system to evaluate the movements of the entire spine, the information provided by the sensors can become redundant, increasing the processing and placement time of all sensors on the subject's back and reducing the patient's comfort by using so many units. Additionally, the reliability of the motion estimation could be compromised depending on the placement site of the sensors. For clinical practice with patients, further research is required to develop new methods to assess the number of sensors needed and their optimal locations for an efficient system that provides accurate and relevant information.

Artificial intelligence (AI) algorithms in the medical field have helped support medical professionals in decision-making based on patient information. Among these algorithms are Machine Learning (ML) models, which, based on a series of features, can perform pattern recognition to make inferences and predictions on new data. Torres-Castillo et al. [32] presented an ML strategy to classify EMG signals to efficiently detect the

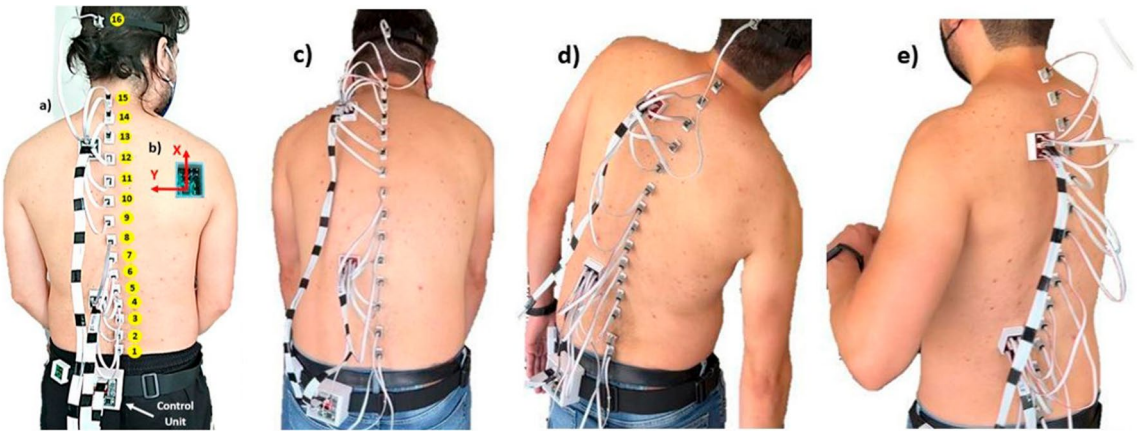

Fig. 1 The system embodiment: **a** MIMUs over the participant's spine; **b** frame reference of the sensors, with the z-axis out of the image. The movements considered in the experimental study: **c** anterior hip flexion; **d** trunk lateral flexions; **e** trunk axial rotation

presence of neuropathy, myopathy, or absence of disease. In [33], Islam et al. quantified physiological biomarkers of a microwave brain stimulation device to predict acute stroke. Regarding inertial sensors and ML algorithms, Kamran et al. [34] use one sensor to detect human posture behaviors and balance, while Moon et al. [35] developed a method to classify Parkinson's disease and essential tremor with six inertial sensors. Other typical applications are gesture recognition and prosthetics control [36] and Ergonomics [37].

Even though these works present the fusion of machine learning algorithms and inertial sensors for the recognition of human movement patterns, to the best of our knowledge, the use of these techniques for the design and optimization of mobility evaluation systems has been little addressed in the literature. Today, there is a need to design specific tools for evaluating spinal mobility with greater capacities than current systems have in terms of the amount of information and specificity.

This work aims to find the optimal configuration of the presented system, enabling an efficient and comprehensive evaluation of the entire spine. The challenge of optimizing sensor placement and data extraction represents a high-dimensional, combinatorial optimization problem. To tackle this, we employed an optimization methodology that relies on ML models to identify the best possible configuration, minimizing the number of sensors while maximizing relevant information. While manual approaches could theoretically process roll, pitch, and yaw data from selected sensors, such methods are limited when handling the complexity and scale of our data. ML models can discern subtle patterns across multiple sensor locations that may not have been obvious through analytical techniques. We eliminate irrelevant and redundant features by automating feature selection through a wrapper approach, improving efficiency and performance. This step is essential because the task's high-dimensional nature complicates manual interpretation and impacts the generalization and computational complexity of traditional methods. Additionally, reducing the dimensionality mitigates the risk of overfitting and lowers data acquisition costs, resulting in a more robust and cost-effective system for spine mobility assessment.

Consequently, reducing the number of sensors on the patient's back and finding its optimal localization is expected to evaluate the entire spine efficiently. Furthermore, the discarded sensors can be used to do a comprehensive assessment of the spine with other articulations of the body like the knees, ankles, shoulders, and arms, which are necessary to evaluate since they can affect the spine movements or be affected by the abnormal movements of the spine.

The main contributions of this work are as follows:

- The optimization of a novel MIMU-based wearable system for mobility assessment that, compared to similar ones, is capable of evaluating the full motion of the spine. This optimization facilitates the clinical practice by reducing the number of sensors, decreasing the time of placement and readback of the system, but preserving the most relevant information of the movements.
- A methodology for optimizing the configuration of sensors of wearable systems for the evaluation of specific movements in different conditions, which represents a complex combinatorial problem of high dimensionality.

This article is organized as follows. Sect. "Materials and Methods" describes the system and methodology

used to perform feature selection, and the Results are presented in Sect. "Results". Then, the advantages and drawbacks of our proposed methodology are discussed in Sect. "Discussion". Finally, the conclusions are drawn in Sect. "Conclusion".

Materials and methods

The strategy to find an optimal configuration of the presented system by selecting the minimum number of sensors and their locations can be summarized in Fig. 2: (a) Acquisition and pre-processing (SubSect. "System description"-"Motion Estimation"), (b) Feature selection strategy (SubSect. "Machine Learning Optimization"), and (c) Configuration selection (SubSect. "Configuration Selection").

System description

As shown in Fig. 1, our wearable system, described in detail in [27], consists of an array of 16 small motion units or MIMUs (Invensense MPU-9250 units, each integrated on a printed circuit board of 11.7 × 9.3 mm). Each MIMU incorporates 9 degrees of freedom (a tri-axial accelerometer, a tri-axial gyroscope, and a tri-axial magnetometer) at a frame rate of 20 Hz. This frame rate is sufficient to capture patient movements with SA because the clinical protocol evaluation involves tasks that require slow execution to ensure safety, minimize the risk of falls or loss of balance, and avoid pain. The first sensor is mounted approximately over the first sacral vertebra (S1), and the fifteenth sensor is located around the seventh cervical vertebra (C7), with an equidistant separation between the fifteen sensors. The sixteenth sensor is mounted with a strap on the head.

Motion estimation

MIMUS has been used for different human mobility assessment applications by estimating the orientation of segments of the human body. However, a well-known issue is the drift problem during the numerical integration of gyroscope signals to obtain rotation angles. To solve this problem, it has been shown that using Kalman filters (KF) allows drift correction by fusing accelerometry and magnetic field signals. A crucial phase of the KF is the statistical calibration of the noise of the gyroscope, accelerometer, and magnetometer signals and the distortion of the latter's signals produced by the surrounding magnetic field [38, 39].

A series of instances of a KF based algorithm estimates the orientation of each MIMU concurrently, with each KF instance explicitly calibrated for each sensor, according to the methodology described in detail in [27]. After the calibration process, we observed an accuracy of 0.8°, which is adequate for human joint mobility estimation. The Euler Angles, roll, pitch, and yaw describe the orientation in the y-, z-, and x-axis, respectively (Fig. 1b).

Machine learning optimization

Movement selection

As outlined earlier, the objective of this study is to identify the optimal ergonomic configuration for the proposed system. To achieve this, the following movements were analyzed (Fig. 1c–e): anterior hip flexion (Mov. 1), trunk lateral flexion (Mov. 2), and trunk axial rotation (Mov. 3). These movements are primarily captured by MIMUs 1 through 15, which are positioned along the spine. Given the number of sensors involved, some redundant information may arise, presenting an opportunity to optimize sensor placement for a more efficient evaluation of the lumbothoracic spine.

Labeling and database implementation

Motion sequences from 12 patients with Ankylosing spondylitis (AS) (10 males, 45.76 ± 11.44 years old, and two females, 52.44 ± 3.53 years old) were obtained using the methodology described in our previous work [27]. The study was approved by the Local Ethics Committee of the General Hospital of Mexico "Dr. Eduardo Liceaga"

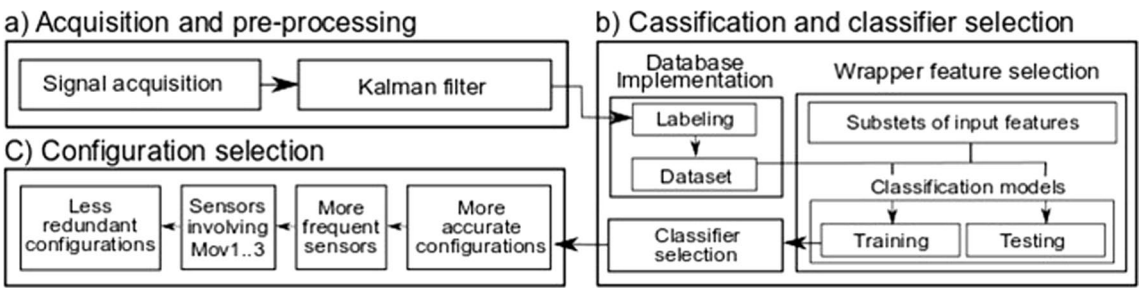

Fig. 2 Block diagram of optimization process: **a** Acquisition and pre-processing; **b** Classification and classifier selection; **c** Selection of optimal MIMU configuration

(protocol code DI/03/17/471). All participants signed the informed consent form.

Two sequences of the three movements were obtained from each patient (Fig. 1c–e): anterior hip flexion, trunk lateral flexions, and trunk axial rotation. Each record has the information of the 15 sensors along the back, which assess the lumbothoracic movements.

Aiming to create a feature array for each movement, data management and labeling of the Range of Motion (RoM) obtained from the 12 patients were necessary. First, an Euler angle (roll, pitch, and yaw) was considered for each movement. According to the reference frame in Fig. 1b, for the Anterior hip flexion (Movement 1), the angle roll describes a greater amplitude than the other two angles. In the case of the Lateral trunk flexion (Movement 2), the pitch angle has a greater amplitude. For the axial trunk rotation (Movement 3), the amplitude is the yaw angle.

As explained above, every participant performed two sequences of each movement. In Fig. 3, the amplitude described by MIMU1 to MIMU15 in a sequence performed by one patient can be observed: (a) Movement 1; (b) Movement 2; (c) Movement 3. Differences in the amplitude of the signals are due to the MIMU's placement; the farther the MIMU is placed from the lumbosacral joint (S1), the greater the amplitude of the RoM.

As shown in Fig. 3, the minimums and maximums of the signals can be clearly distinguished; for anterior hip flexion (Fig. 3a), every maximum represents when the subject is fully flexed, and every minimum represents when the subject is upright. In the case of lateral trunk flexion (Fig. 3b), the minimums represent flexions to the right, and maximums represent flexions to the left. Finally, for axial trunk rotation (Fig. 3c), minimums represent rotations to the right and maximums rotations to the left.

A sample containing the MIMU's signals was considered as a feature instance. In this way, the feature array is formed by the total number of samples (rows) and the signals from the 15 sensors (columns):

$$X_m^s = [x_1; x_2; x_3; \ldots; x_{14}; x_{15}] \quad (1)$$

where X_m^s denotes the feature array for subject $s = 1, \ldots, 15$, and movement $m = 1,2,3$, while the column vectors x_i represent the roll, pitch or yaw angle of the i-th MIMU, of Movements 1 through 3, respectively.

A binary classification was performed for each movement, with two classes defined per movement as follows: (1) maximum extension and flexion for anterior hip movement, (2) maximum right and left flexions for lateral trunk movement, and (3) maximum right and left rotations for axial trunk movement. The average mid-point between adjacent minima and maxima was calculated for all three movements to identify posture transitions and segment the signals into two classes. A label of "1" was assigned to samples representing flexion for Movement 1, and left for Movements 2 and 3. Conversely, a label of "0" was assigned to samples indicating extension for Movement 1, and right for Movements 2 and 3. This procedure was applied to all 72 records: 12 subjects × 3 movements × 2 series.

Dataset description

After labeling, the two sequences for each patient and movement were merged to construct a feature matrix for each subject and movement. Erroneous data, caused by erratic sensor slippage, were manually removed to eliminate outliers. The number of instances obtained for each patient and movement is shown in Table 1. The sample size depends on the duration of the recording and whether one or both motion sequences were retained after exploratory analysis, with the assumption of a roughly equal number of instances per class (0 or 1) for each subject.

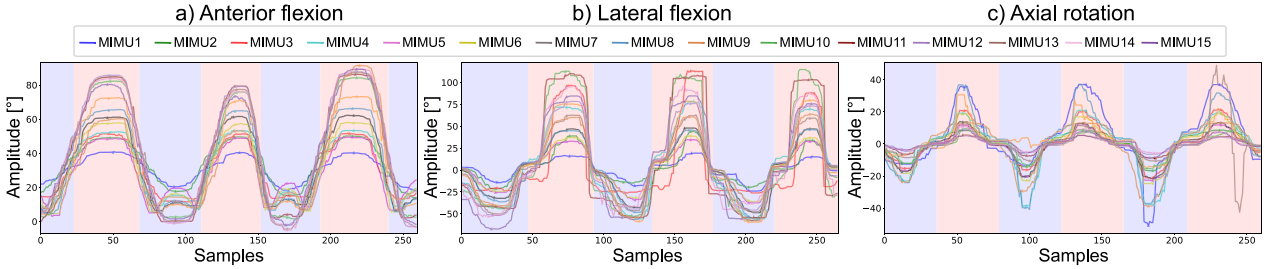

Fig. 3 RoM described by the 15 MIMUs in a sequence of the 3 movements performed by a patient. A different Euler angle describes the amplitude of each movement: **a** roll, **b** pitch, and **c** yaw. A binary classification (0 and 1) was made for every movement. Every sample is determined by the acquisition frequency of the system (i. e., sampling time = 50 ms)

Table 1 Size of the dataset for each patient and movement

	Subjects											
	1	**2**	**3**	**4**	**5**	**6**	**7**	**8**	**9**	**10**	**11**	**12**
Movement 1	640	686	550	495	566	619	350	560	460	–	180	530
Movement 2	325	662	572	603	560	610	540	545	260	530	560	–
Movement 3	260	890	590	754	632	530	330	450	525	255	540	–

The classes of each dataset are balanced, and the datasets of dismissed subjects are marked with a dash

Feature selection

A wrapper feature selection method was carried out, and different subsets of MIMU's configurations were created as input features to select those configurations with the best performance. Two optimizations were applied to generate different subsets of sensors from the 15 available. (i) Constrained optimization (CO): fixing MIMU1 and MIMU15 since MIMU1 is the reference needed to evaluate Movements 1 to 3, and MIMU15 corresponds to the reference used to evaluate movements of the cervical region. Moreover, each subset has at least one sensor placed in the lumbar and thoracic regions to ensure the assessment of all spine regions. ii) Unconstrained optimization (UO): Considering all 15 MIMUs to create the subsets.

Machine learning classifiers

Since the aim of this study is the optimization of the system regardless of the ML method, four of these algorithms were trained and assessed to accomplish a feature selection: (1) Logistic Regression (LR) without added penalty; (2) Naïve Bayes (NB), assuming the likelihood of the features is Gaussian; (3) Support Vector Machine (SVM) with a linear kernel, and (4) K Nearest Neighbor (KNN) with $k = 3$. Hyperparameter tuning was performed by comparing the metric (Sect. "Classification Evaluation") results on the validation set, ensuring the selected configurations provided optimal performance across the models.

Classification training

Leave-One-Subject-Out (LOSO) cross-validation was performed to assess each configuration; this validation consists of training each model with the input dataset of all subjects, leaving one subject out as a test set; then, the method is retrained with all the input datasets leaving out a different subject for testing. This process is applied iteratively for all the available subjects in the data set. The four classifiers mentioned above were used for training and testing: LR, NB, SVM, and KNN.

Classification evaluation

A binary classification (positive or negative) has four possible outcomes. If the instance is positive and is classified as positive, it is counted as a true positive (TP); otherwise, if it is classified as negative, it is counted as a false negative (FN). On the other hand, if the instance is negative and is classified as negative, it is counted as a true negative (TN); otherwise, if it is classified as positive, it is counted as a false positive (FP). Sensitivity (SEN), specificity (SPE), precision (PRE) and accuracy (ACC) were computed to assess the ability of the different MIMUS configurations to discriminate between flexion/extension (Movement 1) and right/left (Movements 2 and 3). A MIMU configuration was considered relevant if it had a high SEN, SPE, PRE, and ACC. The averages of SEN, SPE, PRE, and ACC were calculated from the resulting metrics of each training and testing iteration of the LOSO cross-validation.

Classifier selection

A Multivariate Analysis of Variance (MANOVA) was applied to ACC and PRE metrics following an experimental design of 3 movements (Movement 1, Movement 2, and Movement 3) X 4 classifiers (LR, NB, SVM, and KNN). Then, the Bonferroni honestly Post-hoc test was applied to determine which classifier had the best performance and which movement had the best classification metric. Identifying the movements with the highest classification accuracy allows us to refine sensor positioning, ensuring more stable and reliable measurements while enhancing the system's overall performance.

Configuration selection

After choosing the best classifier, selecting the best configuration was conducted, i.e., the one with the smallest number of sensor units but preserving as much information as possible that allows the discrimination of movements. In other words, the one that, after unit reduction, still efficiently allows the classification of the movements. The process was carried out over Movements 1, 2, and 3.

In each movement, to assess the configurations' performance to discriminate between flexion/extension and right/left, the SEN, SPE, PRE, and ACC metrics of all

obtained configurations were calculated. For both optimizations (UO and CO), the mean of the ACC metric of the configurations in Movement 1 (μ_{ACC_1}), Movement 2 (μ_{ACC_2}), and Movement 3 (μ_{ACC_3}) was calculated. In addition, the standard deviation of the configurations' ACC in each movement was calculated (σ_{ACC_1}, σ_{ACC_2}, σ_{ACC_3}). Finally, from the computed mean and standard deviation, different thresholds were defined as

$$T_{ACC_{i,k}} = \mu_{ACC_i} + \kappa\sigma ACC_i \quad (2)$$

where i corresponds to the three different movements (Movement 1 ($i = 1$), Movement 2 ($i = 2$), and Movement 3 ($i = 3$)) and κ takes the values of $0.5, 1, and 1.5$.

In each movement, three subsets ($S_{i,\kappa}$) of MIMUS configurations were considered, one for each value of κ. The first one includes the configurations whose ACC is greater than $T_{ACC_{i,0.5}} = \mu_{ACC_i}+0.5\sigma_{ACC_i}$; the second subset contains the configurations whose ACC is greater than $T_{ACC_{i,1}} = \mu_{ACC_i}+\sigma_{ACC_i}$; and the last subset considers the configurations whose ACC is greater than $T_{ACC_{i,1.5}} = \mu_{ACC_i}+1.5\sigma_{ACC_i}$.

The frequency $f_{j=1,\ldots,15}$ of the 15 MIMUs in each subset of configurations $S_{i,\kappa}$ was calculated. In other words, we calculated how many times each MIMU appeared in the configurations of a given subset $S_{i,\kappa}$. For example, for CO and Movement 1, we considered the subset of configurations $S_{1,0.5}$ whose ACC was greater than $T_{ACC_{1,0.5}} = \mu_{ACC_1}+0.5\sigma_{ACC_1}$; then, it was computed how many times MIMU1 (f_1) was contained in the resulting configurations, then how many times MIMU2 (f_2) was contained in those same configurations, and so forth up to MIMU15 (f_{15}). This procedure was performed for the two optimizations, the three movements ($i = 1, 2, 3$) and the three thresholds ($\kappa = 0.5, 1, and 1.5$).

For each subset$S_{i,\kappa}$, the median $M_{i,\kappa}$ of all sensor frequencies ($f_{j=1,\ldots,15}$) was calculated for each movement and threshold. The sensors with frequencies greater than the median ($f_j > M_{i,k}$) were considered to form a MIMU configuration ($C_{i,k}$).

At each threshold ($T_{ACC_{i,k}}$), the sensor configurations for the three movements $C_{i,k}$ were compared to derive a final configuration (C_{th_κ}) capable of effectively classifying all three movements. For instance, at the threshold $T_{ACC_{i,0.5}}$, the configurations of the three movements ($C_{1,0.5}, C_{2,0.5}, C_{3,0.5}$) were merged to create a unified configuration that could accurately classify Movements 1 through 3. Sensors that appeared in at least two movements were retained, while those that appeared in only one movement, or not at all, were discarded. The performance of these final configurations was then evaluated using ROC and AUC metrics through LOSO cross validation.

Results

In the feature selection, 326 and 32,767 MIMU configurations were generated by applying CO and UO optimizations, respectively. Four models (NB, LR, SVM, and KNN) were trained and tested on these two feature sets. The models' performance was compared to choose the one that classifies with the best performance. The MANOVA revealed the main factor effects of movements for both ACC ($F(2943) = 2788.138$, $p < 0.00001$) and PRE ($F(2943) = 2317.058$, $p < 0.00001$). The main factor effect was also revealed for classifiers for both ACC ($F(3707) = 5635.967$, $p < 0.00001$) and PRE ($F(3707) = 4226.027$, $p < 0.00001$). Additional interaction was also revealed between both factors for both metrics, $F(6,2820) = 903.931$, $p < 0.00001$ for ACC, while $F(6,2820) = 511.296$, $p < 0.00001$ for PRE. Then the Bonferroni honestly Post-hoc test confirmed better classification metrics for Movement 1, Movement 2, and Movement 3, in this order, while indicating the KNN as the best classifier having the highest ACC for the three movements evaluated. Table 2 presents the ACC and PRE value metrics in the training set for the four classifiers and the three evaluated movements.

The performance of the KNN classifier on the test set, using the CO and UO features, is plotted in Fig. 4. As hundreds and thousands of models were trained for the CO and UO optimizations, respectively, their accuracy distribution is shown. However, it is not possible to explicitly show the configurations and their performance. For both optimizations, it is observed that there is a better classification performance in Movement 1 than for

Table 2 Performance metrics of the classifiers for the three movements, considering Accuracy and Precision of classification

MOV	Accuracy				Precision			
	NB	LR	SMV	KNN	NB	LR	SMV	KNN
1	0.9439 ± 0.0025	0.9494 ± 0.0026	0.9512 ± 0.0027	0.9852 ± 0.0015	0.9553 ± 0.0017	0.9528 ± 0.0023	0.9533 ± 0.0025	1.0 ± 0
2	0.8519 ± 0.0125	0.9053 ± 0.0161	0.9071 ± 0.0148	0.9912 ± 0.0007	0.8539 ± 0.0097	0.9000 ± 0.0162	0.9013 ± 0.0144	1.0 ± 0
3	0.7756 ± 0.0450	0.8991 ± 0.0315	0.9059 ± 0.0268	0.9914 ± 0.0011	0.8040 ± 0.0565	0.8932 ± 0.0354	0.9029 ± 0.0278	1.0 ± 0

A better classification can be observed for Movement 1 (anterior hip flexion), Movement 2 (trunk lateral flexion), and then Movement 3 (trunk axial rotation) with the KNN classifier

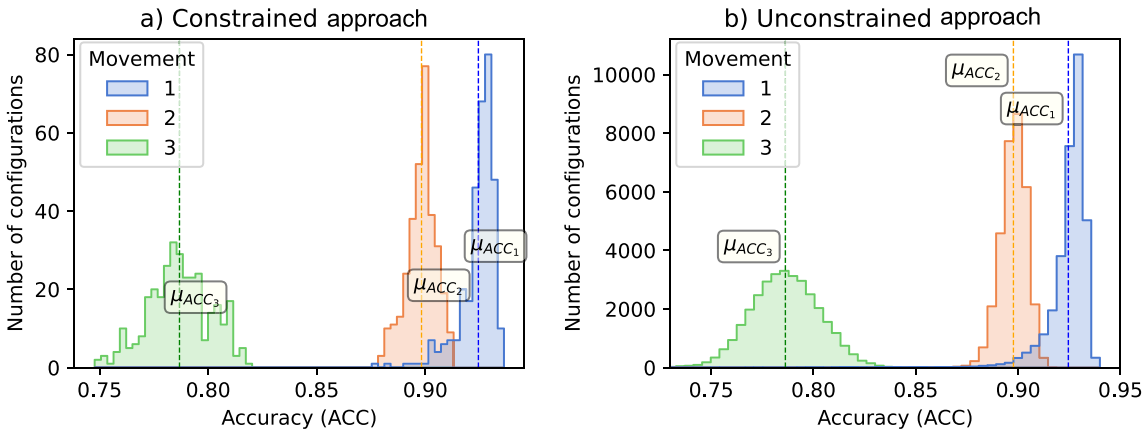

Fig. 4 Accuracy distribution of MIMU configurations for Movement 1 (Anterior Hip Flexion), Movement 2 (Trunk Lateral Flexion), and Movement 3 (Trunk Axial Rotation) using the KNN classifier. The dashed lines indicate the ACC mean of the configurations in each movement. The configurations of MIMUs were generated using two optimizations: **a** The Constrained optimization, where the MIMU1 and MIMU 15 were considered in every configuration; **b** The Unconstrained optimization, where all possible sensor combinations were generated from the 15 available sensors

the other two movements. The dotted lines show the mean of ACC (μ_{ACC_i}) of each distribution.

In each movement, three $T_{ACC_{i,k}}$ thresholds per distribution were defined (*Equation*6). Three configuration sets per movement were considered using the following selection rule: configuration whose performance is higher than the threshold ($ACC > T_{ACC_{i,k}}$) was counted. The frequency of each MIMU in each configuration set is displayed in Fig. 5. Results using CO and UO configurations are shown in Fig. 5a and b, respectively. The sensor frequencies whose $ACC > T_{ACC_{i,0.5}}$ (red bars), $ACC > T_{ACC_{i,1}}$ (green bars), and $ACC > T_{ACC_{i,1.5}}$ (blue bars) are plotted. The dotted lines are the medians of the frequencies of each group. For both CO and UO, there were no configurations with performance greater than $T_{ACC_{1,1.5}}$ in Movement 1.

Sensors with a frequency higher than the median (dashed lines in Fig. 5) were considered to form a new configuration and its classification performance was tested using LOSO cross-validation. Table 3 shows the performance in the test set of the resulting configurations, derived from 2 optimizations (CO and UO) X 3 threshold ($T_{ACC_{i,0.5}}$, $T_{ACC_{i,1}}$, $T_{ACC_{i,1.5}}$) X 3 movements ($i = 1,2,3$).

To obtain a final $C_{i,k}$ configuration involving the 3 movements, the three configurations of a single threshold were compared. Only those sensors that appeared in at least two of the three movements were considered. For the UA, only one configuration in Movement 2 and Movement 3 was considered since there were the same MIMU configuration in the three thresholds; in Movement 1, there were no configurations with performance greater than $T_{ACC_{1,1.5}}$ and for the other two thresholds were the same MIMU configuration. The performance of $C_{i,k}$ configurations in each movement were evaluated through the Receiver Operating Characteristic (ROC) curve and the Area Under the Curve (AUC) by LOSO cross-validation (Table 4).

Table 4 shows that the AUC metrics of the MIMU configuration obtained by UO were higher for the three movements than those obtained by the CO. Thus, the most accurate sensor configurations obtained are:

1) S1: MIMU1, MIMU5, MIMU6, MIMU8, MIMU9, MIMU10, MIMU13, MIMU15.
2) S2: MIMU1, MIMU6, MIMU8, MIMU9, MIMU10, MIMU12, MIMU13, MIMU15.
3) S3: MIMU1, MIMU2, MIMU8, MIMU10, MIMU15.
4) S4: MIMU1, MIMU5, MIMU6, MIMU8, MIMU9, MIMU10, MIMU13, MIMU14, MIMU15

Then, to evaluate possible redundancies among pairs of sensors for each system configuration, a series of analyses of variance (ANOVA) followed by Bonferroni post-hoc tests were applied to compare the RoM measured by the MIMUs for each movement. In this way, redundancy was assumed as any combination of pairs of sensors showing no significant differences in the post-hoc comparison.

The redundancies of S1, S2, S3, and S4 in Movement 1, Movement 2, Movement 3, and the redundancies of using the fifteen sensors are shown in Table 5. It can be observed that the redundancies of the four configurations obtained are approximately a third or less of the redundancies found when all fifteen sensors are used. Based on Tables 4 and 5, although the S4 configuration has a higher number of sensors and more redundancies than the other three configurations, its discrimination

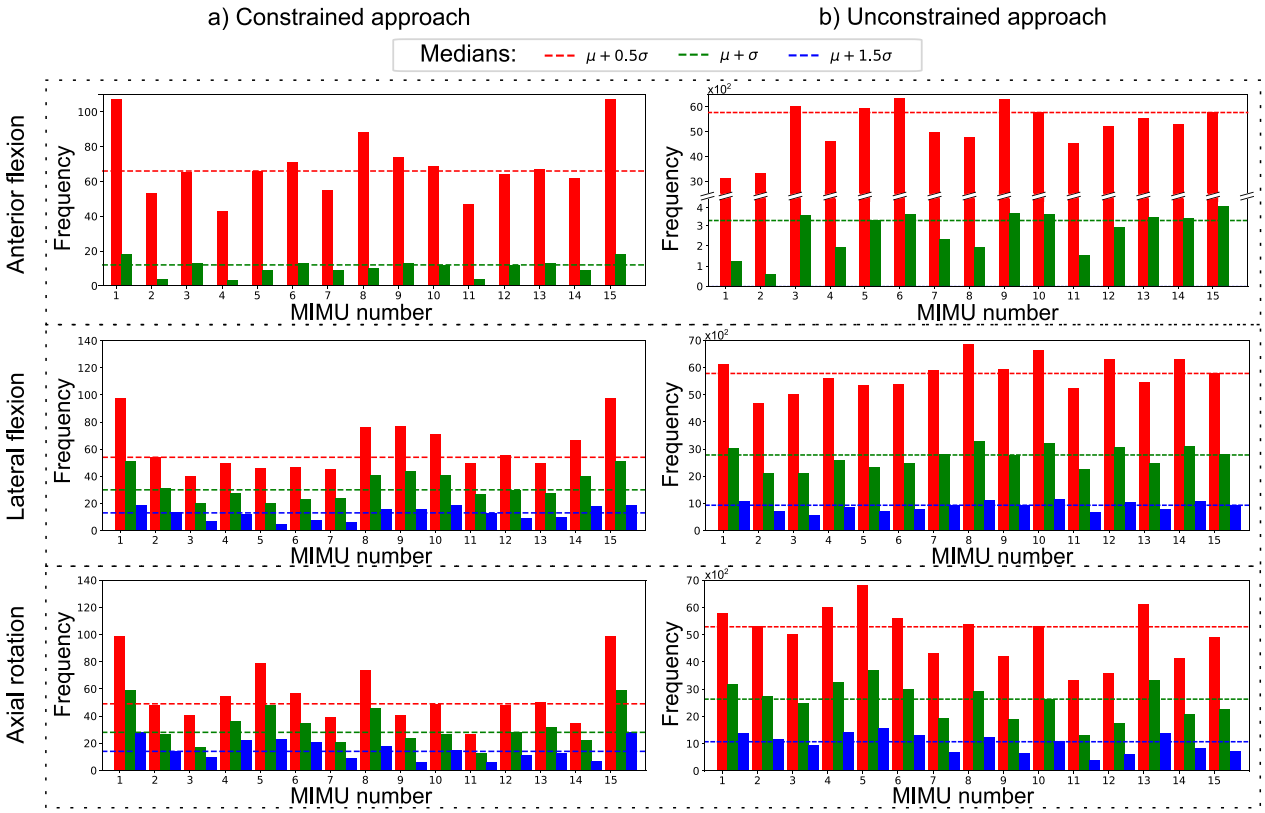

Fig. 5 Sensor frequencies in the configurations with accuracy greater than the threshold: (i)$T_{ACC_{i,0.5}} = \mu_{ACC_i}+0.5\sigma_{ACC_i}$ (red bars); (ii) $T_{ACC_{i,1}} = \mu_{ACC_i}+\sigma_{ACC_i}$ (green bars); (iii) $T_{ACC_{i,1.5}} = \mu_{ACC_i}+1.5\sigma_{ACC_i}$ (blue bars) for the **a** Constrained approach and **b** Unconstrained approach. The frequencies were calculated for Movement 1 ($i = 1$), Movement 2 ($i = 2$), and Movement 3 ($i = 3$). The dashed lines indicate the median of the frequencies of each group

probability (AUC) for the three movements evaluated is higher and has the smallest standard deviation.

Figure 6 shows the ROC response at each movement of the S4 configuration obtained with LOSO cross-validation. Each thin colored line represents the ROC curve of the testing subject used in one of the validation iterations. The thick blue line in the graphs represents the average performance of all the iterations; in each iteration, one different subject's data was considered as a testing set.

Discussion

This study aimed to determine the optimal ergonomic configuration for the system described in [27, 28], which comprises sixteen magnetic and inertial measurement units (MIMUs) designed for the clinical evaluation of spinal mobility in fields such as rheumatology, orthopedics, and rehabilitation. Motion sequences from the three movements involving the thoracic and lumbar spine (Movements 1–3) were analyzed from 12 patients with AS to identify a sensor configuration that captures the most relevant spine mobility information with the fewest necessary sensors. Since MIMUs 1 through 15 are used to evaluate these movements, thousands of possible sensor combinations exist. A wrapper feature selection optimization was implemented to determine the most informative sensor combinations, using different sets of MIMU signals as feature vectors to address this. Two optimizations were employed to generate the sensor configurations: (i) the Constrained optimization (CO), which evaluated 326 configurations with MIMU1 and MIMU15 fixed as reference points, and (ii) the Unconstrained optimization (UO), which explored 32,276 possible configurations utilizing all fifteen available sensors.

Four classifiers were used to evaluate the obtained configurations: two parametric algorithms, (1) Logistic Regression and (2) Naive Bayes; and two non-parametric algorithms, (3) Support Vector Machine and (4) K-Nearest Neighbors (KNN). A Leave-One-Subject-Out (LOSO) cross-validation methodology was used to train and test the classifiers. The LOSO cross-validation methodology is a more robust and accurate estimation of model performance than the usually applied training-test split procedure since all subject data are considered once for testing

Table 3 The most frequent sensors of the most accurate movement configurations

	Movement (i)	Threshold (k) $\mu_{ACC_i} + k\sigma_{ACC}$	MIMU configuration ($C_{i,k}$)	Accuracy (ACC)	Sensitivity (SEN)	Specificity (SPE)
Constrained optimization	1	0.5	1, 5, 6, 8, 9, 10, 13, 15	0.9308 ± 0.0306	0.9420 ± 0.0535	0.9170 ± 0.0513
		1	1, 3, 6, 9, 10, 12, 13, 15	0.9338 ± 0.0282	0.9414 ± 0.0517	0.9243 ± 0.0419
		1.5	–	–	–	–
	2	0.5	1, 2, 8, 9, 10, 12, 14, 15	0.9046 ± 0.0463	0.9173 ± 0.0504	0.8947 ± 0.0783
		1				
		1.5	1, 2, 8, 9, 10, 11, 14, 15	0.9054 ± 0.0432	0.9167 ± 0.0490	0.8978 ± 0.0728
	3	0.5	1, 4, 5, 6, 8, 10, 13, 15	0.8125 ± 0.0905	0.8045 ± 0.1113	0.8262 ± 0.1438
		1	1, 4, 5, 6, 8, 12, 13, 15	0.8162 ± 0.1227	0.8051 ± 0.1705	0.8322 ± 0.1311
		1.5	1, 2, 4, 5, 6, 8, 10, 15	0.8073 ± 0.0882	0.8092 ± 0.1034	0.8117 ± 0.1819
Unconstrained optimization	1	0.5	3, 5, 6, 9, 10, 13, 14, 15	0.9362 ± 0.0230	0.9486 ± 0.0446	0.9216 ± 0.0383
		1				
		1.5	–	–	–	–
	2	0.5	1, 7, 8, 9, 10, 12, 14, 15	0.9009 ± 0.0536	0.9180 ± 0.0647	0.8872 ± 0.0900
		1				
		1.5				
	3	0.5	1, 2, 4, 5, 6, 8, 10, 13	0.8184 ± 0.0717	0.8039 ± 0.0996	0.8383 ± 0.1250
		1				
		1.5				

Three accuracy thresholds $T_{ACC_{i,k}}$ were considered. The metrics ACC, SEN, and SPE for each configuration were calculated

Table 4 Final configurations $C_{i,k}$. The respective AUC calculated from the movement response of the ROC curve is shown

Movement	Threshold	MIMU configuration	AUC for movement 1	AUC for movement 2	AUC for movement 3
Constrained optimization	$\mu_{ACC} + 0.5\sigma_{ACC}$	1, 5, 6, 8, 9, 10, 13, 15	0.960 ± 0.023	0.861 ± 0.199	0.841 ± 0.129
	$\mu_{ACC} + \sigma_{ACC}$	1, 6, 8, 9, 10, 12, 13, 15	0.962 ± 0.027	0.860 ± 0.189	0.834 ± 0.143
	$\mu_{ACC} + 1.5\sigma_{ACC}$	1, 2, 8, 10, 15	0.949 ± 0.036	0.869 ± 0.190	0.843 ± 0.102
Unconstrained optimization	$\mu_{ACC} + 0.5\sigma_{ACC}$	1,5,6,8,9,10,13,14,15	**0.963 ± 0.021**	**0.944 ± 0.038**	**0.852 ± 0.097**
	$\mu_{ACC} + \sigma_{ACC}$				
	$\mu_{ACC} + 1.5\sigma_{ACC}$				

* AUC scores highlighted in bold indicate better performance

Table 5 Redundancies of the four optimal configurations obtained (S1, S2, S3, and S4) for the three movements evaluated and globally

MIMU Configuration	Redundancies for movement 1	Redundancies for movement 2	Redundancies for movement 3	Global redundancies
1, 2, 3, 4, 5, 6, 7, 8, 9, 10, 11, 12, 13, 14, 15	72	100	105	95
1, 5, 6, 8, 9, 10, 13, 15	22	31	34	30
1, 6, 8, 9, 10, 12, 13, 15	23	31	34	29
1, 2, 8, 10, 15	6	8	10	5
1, 5, 6, 8, 9, 10, 13, 14, 15	27	40	43	38

[38, 40]. In addition, LOSO cross-validation is especially useful for assessing generalization across subjects and performing a subject-independent evaluation. Moreover, this methodology makes evaluating the algorithm's behavior on a new subject easier than the training-test splitting procedure. However, the major drawback of the LOSO procedure is the high computational cost since the

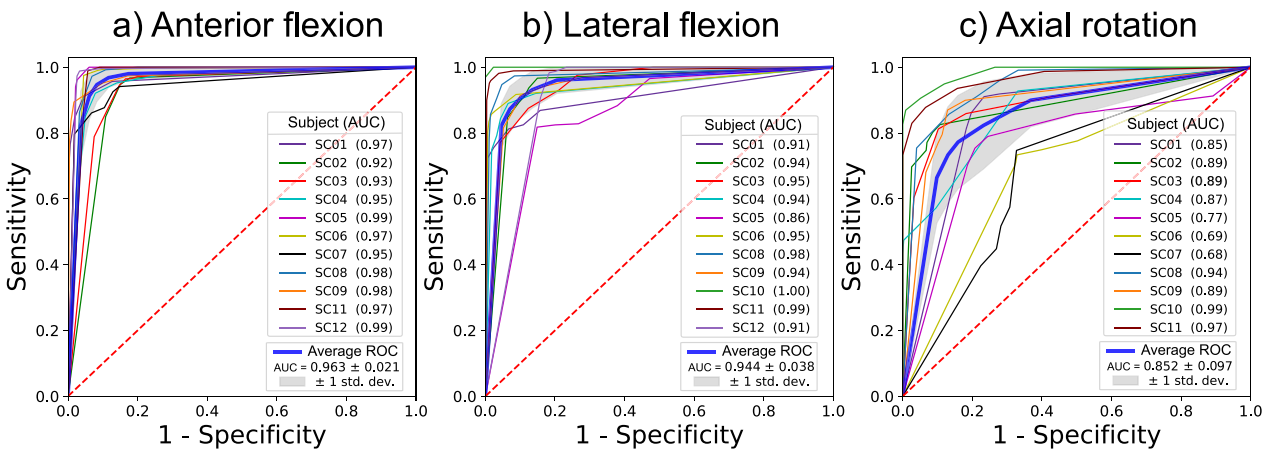

Fig. 6 ROC curves of the configuration S4 (MIMU1, MIMU5, MIMU6, MIMU8, MIMU9, MIMU10, MIMU13, MIMU14, MIMU15) by LOSO cross-validation in the movements: **a** anterior hip flexion; **b** trunk lateral flexion; **c** trunk axial rotation. ROC curves (thin colored lines) represent the performance of the testing set for each iteration. The ROC curve in the thick blue line shows the average performance of the testing set

number of iterations to be performed is increased by the number of subjects to train and test [41].

Table 2 shows the classification metrics of the four proposed ML algorithms, demonstrating better performance with the non-parametric algorithms in each movement. This may be due to parametric methods focus on tuning a few parameters to model the density probability distribution where the data comes from; the chosen density might be a poor distribution model, resulting in low predictive performance. The non-parametric methods freely learn any functional form from the training data, as they do not make strong assumptions about the form of the mapping function; hence, the KNN classifier shows the best performance with the highest accuracy in the three movements. The disadvantages of the non-parametric methods are slow learning and expensive computation.

Since this methodology intends to find a single configuration that allows the best discrimination between flexion/extension (Movement 1) and right/left (Movements 2 and 3), Table 4 shows the most reliable configurations considering the AUC values: S1, S2, S3, and S4 configurations have the best performance over the thousands of configurations acquired. Also noted in Table 4, S4 has the best performance of the four configurations, which consists of nine sensors; this allows a comprehensive assessment of the participant's spine with only the necessary sensors on the back, using the discarded sensors (six) to evaluate other articulations like knees and shoulders, unable to evaluate with the available systems used in previous studies [10, 25, 26].

It is noticed that S4 configuration was obtained with UO, although one limitation of the unconstrained optimization is that it considers all possible combinations that can be formed with the 15 available sensors, causing some evaluated configurations not to consider sensors on the three spine regions, resulting in unnecessary computing calculus; unlike CO, which guarantees to generate configurations with sensors in specific references along the spine.

Even though S4 performs better than S1, S2, and S3, the four obtained configurations have the best performances among all the configurations generated with CO and UO; hence, they can be applied to reliable spine mobility assessment. The choice will depend on the purpose of the study developed; for example, S3 has five sensors, leaving ten (four more than with S4) MIMUs to evaluate other articulations like the knees, feet, or arms.

One limitation of this study is that the signals obtained from the axial trunk rotation present noise due to erratic sliding motions of the sensors caused by the skin deformation during the exercises, which can affect the classification performance for this movement, as seen in Table 4. Even though these sensors with high variability can be considered random, this information is expected to be of little use for discrimination purposes using machine learning techniques; this implies that the optimization tends to discard them from the best-performing configurations. In any case, it is necessary to continue the study with a better positioning configuration of the sensors, like the one presented by Molnar et al. [24], where the sensors were placed on both sides of the spine with less skin displacement.

Another limitation is the number of women who participated in this study because, due to female anatomy, they can develop different RoM compared to males; ten males and two females formed the group. Nevertheless, it is expected since some studies reported a rate of 5:1 of AS affection in males against females [42].

Furthermore, as future work, complementary studies are necessary with more patients with ankylosing spondylitis and the new optimized configuration to validate the system's reliability in the clinical spine evaluation and study the compensatory movements that these patients can develop due to the disease in comparison with a healthy control group; and which can now be assessed with the discarded sensors.

As a final remarkable finding of this methodology, the present study allows finding the minimum number of sensors required to obtain an objective evaluation of the spine, providing more comprehensive information on the biomechanics of the patient's mobility, paving the way for the design of specific instruments for clinical applications.

Conclusion

This work presents a methodology for an information reduction analysis of a system comprised of sixteen MIMUs previously presented by the authors, to obtain an optimal configuration seeking the most relevant information on spine mobility with only the necessary sensors. Four machine learning algorithms were trained and assessed with the data of the RoM in three movements (Mov.1—Anterior hip flexion; Mov.2—Lateral trunk flexion; Mov.3—Axial trunk rotation) obtained from 12 patients with ankylosing spondylitis. This study allowed obtaining a configuration with nine MIMUs on the patient's back, leaving six sensors to evaluate other articulations that can be affected by the disease or due to the compensatory movements, preserving an objective and reliable evaluation of the spine and providing more comprehensive information of the biomechanics of the patients. This can result in a more objective and more timely diagnosis. The information reduction analysis carried out paves the way to design specific systems for particular musculoskeletal disorders or even neurological conditions and for specific anatomical regions or movements.

Acknowledgements
Dalia Yvette Domínguez-Jiménez, Gustavo Pacheco-Santiago, and Adriana Martinez-Hernandez would like to thank the received support for their Master's Degree and Ph.D. studies from CONACYT-Mexico, under the Excellence Grant Program.

Author contributions
Conceptualization: D.Y. D-J, A. M-H, M.A. P–C, and R. B-V. Methodology: D.Y. D-J, A. M-H, M.A. P–C, and R. B-V. Software: D.Y. D-J, A. M-H, G. P-S and M.A. P–C. Validation: D.Y. D-J, A. M-H, G. P-S, J.C. C-V, R. B-V and M.A. P–C. Formal analysis: D.Y. D-J, A. M-H and M.A. P–C. Investigation: D.Y. D-J, A. M-H and M.A. P–C. Resources: M.A. P–C. Data curation: D.Y. D-J, A. M-H, G. P-S, J.C. C-V, R. B-V and M.A. P–C. Writing—original draft preparation: D.Y. D-J, A. M-H, and M.A. P–C. Writing—review and editing: D.Y. D-J, A. M-H, and M.A. P–C. Visualization: D.Y. D-J, A. M-H, and M.A. P–C. Supervision: M.A. P–C and R. B-V. Project administration: M.A. P–C. Funding acquisition: M.A. P–C. All authors have reviewed and agreed to the published this version of the manuscript.

Funding
This research was funded by DGAPA-PAPIIT UNAM, Grant Numbers TA100920 and TA101422, SECTEI Grant Number 219/2019, and SECTEI Grant Number 087/2023.

Data availability
No datasets were generated or analysed during the current study.

Declarations

Institutional review board statement
The study was conducted according to the guidelines of the Declaration of Helsinki and approved by the Ethics Committee and Research Committee of General Hospital of Mexico "Dr. Eduardo Liceaga" (protocol code DI/03/17/471).

Informed consent
Informed consent was obtained from all subjects involved in the study.

Competing interests
The authors declare no competing interests.

Author details
[1]Applied Science and Technology Institute (ICAT), National Autonomous University of Mexico (UNAM), 04510 Mexico City, Mexico. [2]Institute of Applied Research and Technology (InIAT), Universidad Iberoamericana, 01219 Mexico City, Mexico. [3]Rheumatology Service Unit, General Hospital of Mexico "Dr. Eduardo Liceaga", 06720 Mexico City, Mexico. [4]Faculty of Medicine, National Autonomous University of Mexico (UNAM), 04510 Mexico City, Mexico.

Received: 6 February 2024 Accepted: 7 October 2024
Published online: 05 November 2024

References

1. Lemeunier N, et al. Reliability and validity of clinical tests to assess posture, pain location, and cervical spine mobility in adults with neck pain and its associated disorders: Part 4. A systematic review from the cervical assessment and diagnosis research evaluation (CADRE) collaboration. Musculoskelet Sci Pract. 2018;38:128–47. https://doi.org/10.1016/j.msksp.2018.09.013.
2. Sieper J, et al. The assessment of SpondyloArthritis international society (ASAS) handbook: a guide to assess spondyloarthritis. Ann Rheum Dis. 2009;68(Suppl 2):2. https://doi.org/10.1136/ard.2008.104018.
3. Turner KR, Mullan B, Needles N, Stapleton D. Postsurgical therapy for the individual with cerebral palsy. In: Miller F, Bachrach S, Lennon N, O'Neil ME, editors. Cerebral palsy. Cham: Springer International Publishing; 2020. p. 2733–49. https://doi.org/10.1007/978-3-319-74558-9_217.
4. Jenkinson TR, Mallorie PA, Whitelock HC, Kennedy LG, Garrett SL, Calin A. Defining spinal mobility in ankylosing spondylitis (AS). The bath AS metrology index. J Rheumatol. 1994;21(9):9.
5. Abbott JH, Flynn TW, Fritz JM, Hing WA, Reid D, Whitman JM. Manual physical assessment of spinal segmental motion: intent and validity. Man Ther. 2009;14(1):36–44. https://doi.org/10.1016/j.math.2007.09.011.
6. Calvo-Gutiérrez J, et al. Inter-rater reliability of clinical mobility measures in ankylosing spondylitis. BMC Musculoskelet Disord. 2016;17(1):1. https://doi.org/10.1186/s12891-016-1242-1.
7. Hestœk L, Leboeuf-Yde C. Are chiropractic tests for the lumbo-pelvic spine reliable and valid? A systematic critical literature review. J Manip Physiol Ther. 2000;23(4):258–75. https://doi.org/10.1067/mmt.2000.106097.
8. Takatalo J, Ylinen J, Pienimäki T, Häkkinen A. Intra- and inter-rater reliability of thoracic spine mobility and posture assessments in subjects with thoracic spine pain. BMC Musculoskelet Disord. 2020;21(1):529. https://doi.org/10.1186/s12891-020-03551-4.
9. Raya R, et al. An inexpensive and easy to use cervical range of motion measurement solution using inertial sensors. Sensors. 2018. https://doi.org/10.3390/s18082582.

10. O'Grady M, et al. Measuring spinal mobility using an inertial measurement unit system: a reliability study in axial spondyloarthritis. Diagnostics. 2021;11(3):3. https://doi.org/10.3390/diagnostics11030490.
11. Gardiner PV, et al. Validity and reliability of a sensor-based electronic spinal mobility index for axial spondyloarthritis. Rheumatology. 2020;59(11):3415–23. https://doi.org/10.1093/rheumatology/keaa122.
12. Heneghan NR, Webb K, Mahoney T, Rushton A. Thoracic spine mobility, an essential link in upper limb kinetic chains in athletes: a systematic review. Transl Sports Med. 2019;2(6):301–15. https://doi.org/10.1002/tsm2.109.
13. Wirth B, Amstalden M, Perk M, Boutellier U, Humphreys BK. Respiratory dysfunction in patients with chronic neck pain—influence of thoracic spine and chest mobility. Man Ther. 2014;19(5):440–4. https://doi.org/10.1016/j.math.2014.04.011.
14. Kortier HG, Sluiter VI, Roetenberg D, Veltink PH. Assessment of hand kinematics using inertial and magnetic sensors. J NeuroEng Rehabilit. 2014;11(1):70. https://doi.org/10.1186/1743-0003-11-70.
15. Nguyen HP, et al. Auto detection and segmentation of physical activities during a timed-up-and-Go (TUG) task in healthy older adults using multiple inertial sensors. J NeuroEng Rehabilit. 2015;12(1):36. https://doi.org/10.1186/s12984-015-0026-4.
16. Revi DA, Alvarez AM, Walsh CJ, De Rossi SMM, Awad LN. Indirect measurement of anterior-posterior ground reaction forces using a minimal set of wearable inertial sensors: from healthy to hemiparetic walking. J NeuroEng Rehabilit. 2020;17(1):82. https://doi.org/10.1186/s12984-020-00700-7.
17. Milosevic B, Leardini A, Farella E. Kinect and wearable inertial sensors for motor rehabilitation programs at home: state of the art and an experimental comparison. BioMed Eng OnLine. 2020;19(1):25. https://doi.org/10.1186/s12938-020-00762-7.
18. Kobsar D, Osis ST, Boyd JE, Hettinga BA, Ferber R. Wearable sensors to predict improvement following an exercise intervention in patients with knee osteoarthritis. J Neuroeng Rehabil. 2017;14(1):94. https://doi.org/10.1186/s12984-017-0309-z.
19. Gholipour A, Arjmand N. Artificial neural networks to predict 3D spinal posture in reaching and lifting activities applications in biomechanical models. J Biomech. 2016;49(13):2946–52. https://doi.org/10.1016/j.jbiomech.2016.07.008.
20. Papi E, Koh WS, McGregor AH. Wearable technology for spine movement assessment: a systematic review. J Biomech. 2017;64:186–97. https://doi.org/10.1016/j.jbiomech.2017.09.037.
21. Simpson L, Maharaj MM, Mobbs RJ. The role of wearables in spinal posture analysis: a systematic review. BMC Musculoskelet Disord. 2019;20(1):1. https://doi.org/10.1186/s12891-019-2430-6.
22. Fathi A, Curran K. Detection of spine curvature using wireless sensors. J King Saud Univ Sci. 2017;29(4):553–60. https://doi.org/10.1016/j.jksus.2017.09.014.
23. Mjøsund HL, Boyle E, Kjaer P, Mieritz RM, Skallgård T, Kent P. Clinically acceptable agreement between the ViMove wireless motion sensor system and the Vicon motion capture system when measuring lumbar region inclination motion in the sagittal and coronal planes. BMC Musculoskelet Disord. 2017;18(1):124. https://doi.org/10.1186/s12891-017-1489-1.
24. Molnar M, Kok M, Engel T, Kaplick H, Mayer F, Seel T, A Method for lower back motion assessment using wearable 6D inertial sensors. 2018. https://doi.org/10.23919/ICIF.2018.8455828.
25. Aranda-Valera IC, et al. Measuring spinal mobility using an inertial measurement unit system: a validation study in axial spondyloarthritis. Diagnostics. 2020. https://doi.org/10.3390/diagnostics10060426.
26. Franco L, Sengupta R, Wade L, Cazzola D. A novel IMU-based clinical assessment protocol for Axial Spondyloarthritis: a protocol validation study. PeerJ. 2021;9: e10623. https://doi.org/10.7717/peerj.10623.
27. Martínez-Hernández A, Perez-Lomelí JS, Burgos-Vargas R, Padilla-Castañeda MA. A wearable system based on multiple magnetic and inertial measurement units for spine mobility assessment: a reliability study for the evaluation of ankylosing spondylitis. Sensors. 2022. https://doi.org/10.3390/s22041332.
28. Martínez-Hernández A, Pérez Lomeli JS, Casasola-Vargas J, Padilla-Castañeda MA, Burgos-Vargas R. Evaluation of the spine mobility in patients with ankylosing spondyloarthritis through a novel multi-sensor inertial system: a pilot test, en PANLAR 23rd congress abstracts. J Clin Rheumatol. 2021. https://doi.org/10.1097/RHU.0000000000001781.
29. Rudwaleit M, et al. The development of assessment of SpondyloArthritis international society classification criteria for axial spondyloarthritis (part I): classification of paper patients by expert opinion including uncertainty appraisal. Ann Rheum Dis. 2009;68(6):6. https://doi.org/10.1136/ard.2009.108217.
30. Rudwaleit M, et al. The development of assessment of SpondyloArthritis international society classification criteria for axial spondyloarthritis (part II): validation and final selection. Ann Rheum Dis. 2009;68(6):6. https://doi.org/10.1136/ard.2009.108233.
31. Koo TK, Li MY. A guideline of selecting and reporting intraclass correlation coefficients for reliability research. J Chiropr Med. 2016;15(2):155–63. https://doi.org/10.1016/j.jcm.2016.02.012.
32. Torres-Castillo JR, López-López CO, Padilla-Castañeda MA. Neuromuscular disorders detection through time-frequency analysis and classification of multi-muscular EMG signals using Hilbert-Huang transform. Biomed Signal Process Control. 2022;71:103037. https://doi.org/10.1016/j.bspc.2021.103037.
33. Islam MS, Hussain I, Rahman MM, Park SJ, Hossain MA. Explainable artificial intelligence model for stroke prediction using EEG signal. Sensors. 2022;22(24):24. https://doi.org/10.3390/s22249859.
34. Kamran F, et al. Automatically evaluating balance using machine learning and data from a single inertial measurement unit. J NeuroEng Rehabilit. 2021;18(1):114. https://doi.org/10.1186/s12984-021-00894-4.
35. Moon S, et al. Classification of Parkinson's disease and essential tremor based on balance and gait characteristics from wearable motion sensors via machine learning techniques: a data-driven approach. J NeuroEng Rehabilit. 2020;17(1):125. https://doi.org/10.1186/s12984-020-00756-5.
36. Jiang S, et al. Feasibility of wrist-worn, real-time hand, and surface gesture recognition via sEMG and IMU sensing. IEEE Trans Ind Inform. 2018;14(8):3376–85. https://doi.org/10.1109/TII.2017.2779814.
37. Chan VCH, Ross GB, Clouthier AL, Fischer SL, Graham RB. The role of machine learning in the primary prevention of work-related musculoskeletal disorders: a scoping review. Appl Ergon. 2022;98:103574. https://doi.org/10.1016/j.apergo.2021.103574.
38. Chowdhury AK, Tjondronegoro D, Chandran V, Trost SG. Physical activity recognition using posterior-adapted class-based fusion of multiaccelerometer data. IEEE J Biomed Health Inform. 2018;22(3):678–85. https://doi.org/10.1109/JBHI.2017.2705036.
39. Lee JK, Park EJ, Robinovitch SN. Estimation of attitude and external acceleration using inertial sensor measurement during various dynamic conditions. IEEE Trans Instrum Meas. 2012;61(8):2262–73. https://doi.org/10.1109/TIM.2012.2187245.
40. Gholamiangonabadi D, Kiselov N, Grolinger K. Deep neural networks for human activity recognition with wearable sensors: leave-one-subject-out cross-validation for model selection. IEEE Access. 2020;8:133982–94. https://doi.org/10.1109/ACCESS.2020.3010715.
41. Bishop CM. Pattern recognition and machine learning. In: Information science and statistics. New York: Springer; 2006.
42. Burgos-Vargas R, Peláez-Ballestas I. Epidemiology of spondyloarthritis in México. Am J Med Sci. 2011. https://doi.org/10.1097/MAJ.0b013e31820f8d0a.

Publisher's Note